Detection of Himalayan thar using a thermal infrared camera

R H Wilde and C M Trotter
Land Management Group
Landcare Research
Private Bag 11-052
Palmerston North
New Zealand

Published by
Department of Conservation
Head Office, PO Box 10-420
Wellington, New Zealand

This report was commissioned by West Coast Conservancy

ISSN 1171-9834

Reference to material in this report should be cited thus:

Wilde, R.H. and Trotter, C.M., 1999
Detection of Himalayan that using a thermal infrared camera Conservation Advisory Science Notes No. 223, Department of Conservation, Wellington.

Keywords: Himalayan that, thermal infrared camera, animal detection

Abstract

The thermal characteristics of thar and their alpine habitat (including expanses of bare rock) were determined as a function of time throughout the night, by measurements from imagery acquired with a thermal video camera. Measurements were also made on thar in a farm environment, to determine the radiant temperature difference between their considerably hotter heads and cooler bodies.

Thermal infrared (TIR) imaging for detection of thar in an alpine environment should not be attempted until about six hours after sunset, to allow time for rocks to cool sufficiently. Ideally, imaging should be carried out from a few hours before dawn until about one hour after sunrise. At these times, and under the conditions encountered in this study (thar at a distance such that pixel sizes of about 40 cm square were encountered), moving thar will be easily detected.

It is highly probable that stationary thar in an alpine environment could be detected with a high degree of reliability, on the basis of radiant temperature alone, if pixel sizes equivalent to imaging areas of 20 cm square could be used. These pixel sizes approximate the dimensions of a thar head, which is relatively hot.

Thar moving in an alpine environment can probably be unambiguously detected with current TIR cameras operating from an aircraft, if the aircraft disturbs the animals and causes them to run about. However, cameras available in New Zealand will only allow limited swath widths to be covered (c. 100 m).

As the use of TIR imaging for operational detection of thar has much in common with detection of possums, it should be possible to share the development cost of any operational system for TIR imaging across a range of animal population estimation applications (probably also including such animals as chamois, deer, seals, albatross, etc.).

1. Introduction

Existing methods of visually indexing the abundance of thar have significant limitations, and improved methods are required to meet DoC's objective of controlling animal numbers so that "unacceptable damage to conservation values is avoided" (Forsyth & Hickling 1997). This study was carried out to determine the feasibility of using thermal infrared (TIR) imaging to detect and count thar in an alpine environment, by providing basic information about the thermal characteristics of thar and thar habitat. To date, there have been no studies quantifying either the radiant temperature of thar relative to their environment or the radiant temperature and cooling rates of their environment. As a consequence, very little is known about TIR imaging as a means of detecting thar.

1.1 BRIEF OVERVIEW OF THE BASIS FOR TIR IMAGING

All objects at the earth's surface are heated daily by the sun's radiant energy. They, in turn, lose heat through conduction, convection to the surroundings, and radiation of thermal energy to the atmosphere.This radiant heat loss, detected by appropriate instrumentation, is the basis of TIR imaging.

The ability of an object to radiate heat depends both on its surface temperature, and on its surface characteristics as quantified by the parameter termed 'thermal emissivity' (e.g. a white object radiates less heat than a black object of the same type at the same temperature, and so the white object has a lower thermal emissivity). Most natural objects (leaves, fur, rocks, etc) have very similar values of thermal emissivity (Birkebak et al. 1964; Guoquan & Zhengzhi 1992). For all practical purposes, therefore, it is simply the difference between the object's surface temperature and that of its surroundings that determines the radiant heat loss. The main requirement for detecting a natural object by TIR imaging is that the surface temperature of the object must exceed the temperature of its surroundings, so that there is thermal contrast between the object and its surroundings. (The surroundings are also termed the 'thermal background', or just `background'.) A more general term for surface temperature is radiant temperature, and we shall use this term throughout the remainder of the report.

A TIR imaging device (e.g. a TIR video camera) produces an image in a way exactly analogous to forming images from visible light with familiar electronic imaging devices like video or digital cameras. Thermal cameras contain an array of detectors that convert thermal energy to an electrical output signal whose amplitude is proportional to the amount of energy detected. This output signal can be processed as a normal video signal, stored on video tape, and later displayed on a video screen as a grey-scale image of the scene. The grey-scale value in the images represents the amount of thermal energy detected from a given point in the scene and is proportional to the radiant temperature of that point. Hotter radiant temperatures are normally displayed as whiter tones in an image, and colder temperatures as blacker tones.

Animals maintain optimum body temperatures by balancing metabolic activity with their energy demands from activity and heat loss. It is the heat loss component radiated by the animal that is detected by TIR imaging. Apart from variations in thermal insulation (thickness and cover of hair coats), an animal can regulate its heat loss by: standing or lying down to vary its exposed surface area; muscular activity; diet; variable hair insulation through piloerection; and seeking shelter (Moen 1991). Any of these activities may affect the amount of heat radiated by the animal. If the radiant temperature of animals is several degrees above that of their local surroundings, they can generally be detected by TIR imaging, provided they are not masked from the view of the imaging device by vegetation, which effectively blocks thermal energy.

1.2 REVIEW OF ANIMAL DETECTION USING THERMAL INFRARED TECHNIQUES

Thermal imaging for animal detection and census is still in its early stages in New Zealand. To date, we are aware of only two studies performed on possums (Dymond & Trotter 1996, Halverson 1994), and one qualitative inspection of seals (J. R. Dymond *pers. comm.*). Overseas, however, thermography has been used extensively to detect a range of animal species: deer (Graves *et al.* 1972; Wiggers & Beckerman 1993; Croon *et al.* 1968); bats (Sabol & Hudson 1995; Kirkwood & Cartwright 1991; Kirkwood & Cartwright 1993); squirrels, hares, and mice (Boonstra *et al.* 1994); and birds (Boonstra *et al.* 1995; Sidle *et al.* 1993). Boonstra *et al.* (1995) successfully detected empty nest sites using ground-based thermography. Boonstra *et al.* (1994) found that small mammals could be easily detected with ground-based thermography and suggested early morning as the best time to obtain the maximum temperature difference between mammals and their surroundings (also referred to as 'the background').

Using aerial thermography, Graves et *al.* (1972) found that the ability to detect deer in non-forest conditions depended on the time of day, season, altitude, and thermal wavelength. They recommended that imaging be done at night to maximise the temperature difference (thermal contrast) between deer and the background, and that 3-14 μm detectors be used in winter, and 3-5 μm detectors in summer. Croon *et al.* (1968) found that deer in non-forest conditions could be counted accurately from aerial thermography, but warned of difficulties in forest situations because thermal infrared radiation is unable to penetrate green leaf canopy. Wiggers & Beckerman (1993) also determined that deer could be accurately counted from aerial thermography in non-forest situations. Detection of cranes on water using aerial thermography has been successfully carried out by Sidle *et al.* (1993).

Because the thermal emissivities of natural materials are essentially the same (Birkebak *et al.* 1964; Guoquan & Zhengzhi 1992), the detectability of animals when using thermography is controlled primarily by the radiant temperature difference between the animal and its surroundings. There have been a number of experimental studies to determine this temperature difference: Croen *et al.* (1968) measured the average temperature difference between deer and the background to be 7°C; Moen *(1984)* found the difference to be between 6°C and 8°C for white-tailed deer; De Lamo & Heath (1985) measured a 3°C difference on the fur of llamas; Best (1981) measured the temperature difference of Canada geese to be 6°C and 3°C (at 0°C and 10°C, respectively); and Webb *et al.* (1993) measured the difference to be 20°C and 15°C (at 0°C and 10°C, respectively) for brown long-eared bats. In terms of the spatial distribution of heat loss, both Klir & Heath (1992) and Korhonen & Harri (1986) found that radiant heat loss from foxes was highly variable over the animal surface, with most loss coming from the chest, head, abdomen, and feet.

Despite these studies, a theoretical framework for detection of animals by aerial thermography (i.e. predicting the difference between animal and background radiant temperatures, as a function of background temperature) has only recently been formalised and verified in a study on possums (Dymond &

Trotter 1996). They calculated that for possums, the temperature difference on still nights was over 4 °C and was largely independent of either the average ambient temperature or the season. They supported their calculations with experimental work, and also found that the temperature difference between possums and their background environment is sufficient for unambiguous detection using currently available TIR cameras, provided that the possums are in full view of the camera.

Dymond & Trotter (1996) recommended that TIR imaging of possums should ideally be carried out on nights with little wind, beginning at least one hour after sunset on clear nights and two hours after sunset on cloudy nights. This allows sufficient time for hotspots in the forest canopy to cool, as these would otherwise be confused with possums.

2. Objectives

The study had two objectives:

- To determine the thermal characteristics of thar and their alpine habitat (including expanses of largely bare rock) as a function of time during the night, so that a definitive statement can be made about their detectability under conditions likely to be encountered during operational surveys of animal numbers.

- To determine the thermal characteristics of chamois and hares, and to compare thermal characteristics of chamois and char to see if they are distinguishable in thermal imagery.

This second objective depended on two conditions: chamois being visible at distances similar to thar; and hares being present within about 300 m of the camera. Unfortunately, no chamois or hares were seen during fieldwork, although plenty of hare sign was seen at the observation site. It was, therefore, possible to complete only the first objective.

The single output for this contract consists of this report which describes:

- the equipment and its use in the project;

- the thermal characteristics and cooling rate of thar habitat, and its influence on thar detectability;

- detection of thar in the alpine environment;

- the radiant temperature distribution over (female and juvenile) thar bodies.

3. Method

3.1 EQUIPMENT

The thermal infrared camera used for this study was a **Prism™** DS camera manufactured by FLIR Systems Inc 16505 SW 72rd Avenue, Portland, Oregon 97224, USA. Specifications are given in Table 1.

The output from the camera is a video signal, which was recorded on a good quality VHS video cassette recorder (Sony model SLV-X822) running off a 12 to 230 V inverter powered by two sealed lead-acid batteries. Monitoring of the camera output was done using a 12 V video display with a 10-inch screen. The camera was powered directly from the 12 V batteries, which were recharged from a petrol generator. In the field, the camera, recorder, video monitor, and batteries were housed in a tent to prevent condensation forming on the equipment and camera lens.

3.2 STUDY AREA AND IMAGING SITES

The fieldwork phase of the study was carried out on 11-12 April 1997 in the headwaters of the Douglas River, South Westland, close to the main divide of the Southern Alps and about 27 km SSW of Fox Glacier Township. The grid reference is 2262900, 5718700 on NZMS 260 Sheet H36 (Mt Cook).

The weather during the evening of 11 April and early morning of 12 April was clear and cloudless with moderate frost and no wind, providing optimum conditions for radiant heat loss from thar and from the rocky landscape. Sunrise and sunset on 11 April were close to 0705 hours and 1810 hours respectively (NZ Nautical Almanac, 1997).

The observation point where the equipment was set up was situated in a grassy clearing on the flat top of a scrub-covered moraine wall at 980 m elevation. Below 1100 m the thin soil supports scrub vegetation, and there is tussock above 1100 m. South-east of the observation point, the tussock and rock covered slopes lead to a bare rocky ridge at about 2000 m elevation, defined by Mt Gladiator in the north-east and Mt Howitt in the south-west. South and south-west of the observation point, very steep bluffs lead to the Pommell at 1791 m elevation and Red Deer Col at 1570 m.

Two areas frequently grazed by thar were selected as imaging sites on the advice of staff of the Wild Animal Control Section, Department of Conservation, Hokitika. One area, south-east of the observation point and about 1 square kilometre in area comprised rocky, tussock-covered moderately steep **(25°)** slopes extending from the scrub line at approximately 700 m from the observation site, to the bottom of prominent bluffs at approximately 1100 m from the observation site. This grazing area was imaged by tilting the camera no more than **22°** above the horizontal.

The second imaging site, south-west of the observation point, comprised very steep bluffs (63° slopes) with many tussock-covered ledges. The bottom of the bluffs was about 200 m from the observation point and the midslopes about 600 m away. Inclining the camera at an angle of 33° above the horizontal allowed the midslopes to be imaged. With such a steep camera angle, only thar grazing along the outer margins of rock ledges were visible to the camera.

For a given focal length lens, pixel size depends on imaging distance. The image in the Prism DS camera is 320 pixels wide by 244 high, and the lens used had a focal length of 50 mm (Table 1). At a distance of 800 m using this lens, this corresponds to each pixel imaging an area of 384 mm by 384 mm (see Table 2, which also contains the area imaged at other distances). The further the camera is from an animal, the larger is the area viewed by each pixel, with fewer pixels per animal, and more pixels comprising a mixture of warm animal and cooler background thermal values. Pixels containing such mixtures will obviously not be as bright (white) as those containing parts of the animal's body only.

For this project, we estimated that to image thar successfully they should be within 800 m of the observation site so that some pixels were always completely filled by the animal. It was also desirable for some animals to be 1000 m away to test whether thar could be seen at this distance. Thar in the alpine environment imaged during the study were between 700 m and 1100 m, although most observations were made at around 950 m from the camera. This slightly exceeded the recommended distances specified in the contract, and thar appeared as somewhat smaller objects in the images than was ideal.

3.3 THERMAL IMAGING AND ANALYSIS

Thermal imaging was carried out shortly before sunset at 5.45 p.m. on 11 April to test the equipment and to obtain radiant temperatures of rocks and vegetation early in the evening. Imaging was again carried out from 6.50 p.m. until 7.00 p.m., from 8.00 p.m. until 9.00 p.m., and from 10.30 p.m. until 4.00 a.m. the next morning. Imaging resumed at 4.30 a.m. and continued until 5.45 a.m., when the batteries needed recharging, and continued once again from 6.45 a.m. until 7.00 a.m. After one hour further charging, imaging was carried out from 8.00 a.m. until 8.15 a.m., when the battery voltage finally became too low for camera operation.

During thermal imaging in the alpine environment, thar could only be easily distinguished from the warm surrounding rocks when they moved. To obtain representative image frames showing thar, the camera was panned over the areas most likely to contain grazing thar while continuously monitoring the camera output to detect any thar movement. When animals were observed, their locations on the video tape were noted in relation to the central cross-hairs (see Figure 2). Also noted was the time recorded on the video images.

Imaging of thar to obtain relative radiant temperatures of thar heads and bodies was carried out between 6.00 p.m. and 6.30 p.m. on 12 April, at a farm

location near Hokitika. The observation point was sited approximately 150 m from the animals.

A total of 6.5 hours of video tape imaging were acquired of thar in alpine and farm environments. In the laboratory, the video tapes were played back with the same VCR used for recording, and viewed on a 12-inch video monitor. Selected frames were digitised using Epix, a PC-based image processing package. Subsequent image display and analysis were carried out using Imagine software running on a Sun workstation.

4. Results and discussion

4.1 COOLING RATE OF THAR HABITAT, AND ITS INFLUENCE ON THAR DETECTABILITY

In regulating their own heat loss, and thus their radiant temperature, thar will react to the average temperature of their surroundings. In these surroundings there will be objects that have retained heat from direct heating by the sun earlier in the day, and these may well be considerably hotter (and have a higher radiant temperature) than the average temperature of the surroundings. Before attempting detection of thar by thermal imaging, therefore, it is necessary to allow time for objects, particularly those with a high heat capacity (like rocks and also any thick woody stems or large branches of scrub, if these are visible), to cool to temperatures approaching the average environmental temperature. In the alpine environment, it will be necessary to wait at least until the cooling rates of rocks have become constant. This will ensure that local temperature gradients have largely dissipated, and that a relatively uniform temperature is established over as wide a local area as possible.

Figure 1 provides data from which this time can be determined. It shows typical changes in rock temperature (both modelled, and where possible measured) in response to diurnal solar heating. The data indicate that the rate of cooling does not reduce much after 11 - 12 p.m., and local temperature gradients are, therefore, unlikely to get much smaller after this time. Because sunset on the date of imaging occurred at 6.10 p.m., detection of thar should, therefore, be scheduled to start no earlier than 5-6 hours after sunset.

4.2 DETECTION OF THAR IN THE ALPINE ENVIRONMENT

A thermal image of the general alpine environment, including a thar, is shown in Figure 2. Typical data showing the radiant temperature of thar in comparison with temperatures present in the area covered by a single video frame (approximately 1.2 ha) are shown in Figure 3. The data cover the period between 11 p.m. and 8.15 a.m., and show thar radiant temperatures are well above the mean radiant temperature of the environment during this period. However, the data also show that, at all times, a small fraction of the alpine

environment exhibits radiant temperatures greater than observed thar radiant temperatures. These areas of the landscape would be mis-identified as thar, if identification was based on radiant temperature values alone. However, when the camera was pointing at a fixed area, thar were quite easy to detect because they moved about and provided a varying thermal contrast at the points they occupied in the image.

For the set of 48 observations made of thar, the statistics relating to the percentage of pixels in a single video frame that show higher radiant temperatures (i.e. the brightness levels) than thar are given in Table 3. Initial reaction to the data indicates that the potential to mis-identify objects in thermal imagery as thar is quite high, should identification be based on temperature alone. Even if we take the median situation as typical, there are on average many (1500) pixels in an image brighter than thar.

It is notable that the radiant temperatures measured for thar apparently show a significant range. This is unexpected, as animals generally exhibit a fairly constant radiant temperature (for a given state of activity). However, it was suspected before this study, and has been confirmed as part of this work (see section 5.3), that the radiant temperature of different thar body areas varies significantly, with the head being considerably hotter than the body. (This is likely to be especially true for male thar in winter, given their seasonally thick, shaggy, coats.) The variation observed in thar radiant temperature in the alpine environment and recorded in Table 3 is, therefore, attributed largely to variation in the percentage of head visible to the thermal camera. Detectability (radiant temperature difference between thar and the background) would, therefore, have been strongly dependent on how the animal was standing in relation to the camera.

We can conclude from these alpine environment measurements that radiant temperature of thar bodies (i.e. head excluded) is not sufficiently high to identify them adequately, based solely on radiant temperature. The minimum value recorded in Table 3 probably represents detectability when only the bodies are visible to the camera. The maximum value probably represents detectability when the thar was standing looking directly at the camera, with the largest proportion of head visible. Other radiant temperatures recorded for thar will represent situations between these two extremes. In addition, because the head is much smaller than the dimensions of a pixel (38 cm square at 800 m from the camera - see Table 2), the true radiant temperature of the head would never have been measured. If pixel sizes closer to the head dimensions were used, detection could be much improved.

4.3 RADIANT TEMPERATURES OF THAR IN THE FARM ENVIRONMENT

There was an opportunity during the study to obtain relatively close-up thermal images of thar in a farm environment. Imaging was performed under these conditions to improve understanding of radiant temperature distribution over the animal. The on-farm thermal imaging of thar was carried out on the evening of 12 April at a location near Hokitika, with the camera placed

approximately 150 m from the animals to obtain actual radiant temperature measurements of thar heads in relation to body radiant temperature.

Mean temperatures of 14°C for heads and 11°C for bodies were calculated from the imagery. The farm environment (c.150 m elevation) was considerably lower than the alpine habitat (c.1300 m), and the background temperature (vegetation) was estimated from the imagery to be approximately 4°C. This placed the heads at 10°C and the bodies at 7°C above the background temperature. A radiant temperature for thar bodies of 7°C above the background temperature is similar to that expected for deer (Croen *et al.* 1968). A typical thermal image of thar in this environment is shown in Figure 4. Only female and juvenile thar were available for observation, so body radiant temperatures measured here are probably higher than for male thar which have a thicker coat. As shown in Figure 4, the heads of thar are the brightest parts of the body (radiating most heat) because they are least insulated and have a high blood flow.

4.4 IMPROVEMENT IN DETECTION OF THAR USING SMALLER PIXEL SIZES

Because the heads of thar have a significantly higher radiant temperature than their bodies,TIR detection could be improved by using an image pixel size more closely approximating the head size. There is a disadvantage in reducing the pixel size in that the camera then images a smaller total area. In the context of aerial survey, this means that as the pixel size decreases smaller swath widths will be covered. However, thermal camera technology is advancing rapidly, and cameras with three times the pixel resolution of the camera used here are already available, while newer systems with up to five times the resolution are planned. Such advanced cameras would allow significant swath widths to be maintained even with small pixel sizes: for example, a 300 m swath with a ground resolution (pixel size) of 20 cm is expected to be achievable in the near future. If reasonable swath widths (and thus total area coverage) are to be maintained, it is probably not feasible to reduce pixel size significantly below 20 cm. If surveys with a helicopter-mounted TIR camera cause thar to startle, thar may be detectable with pixel sizes of up to about 40 cm, since moving animals are much simpler to identify in TIR imagery than stationary ones.

To estimate the improvement in detection of thar at smaller pixel sizes, it is necessary first to calculate the percentage of the pixel area occupied by a thar's head. Area measurements of thar heads (Table 4) were made from a mount of a large male (Terry Farrell, DoC, 1997, *pers. comm.)* and also calculated from a photograph and measurements of thar given in Tustin (1990).

Table 5 gives data on the percentage of a pixel occupied by a thar head, for two pixel sizes: 38 cm, as nominally achieved in the alpine environment section of this study (with an observation distance of 800 m), and about half this size, 20 cm, representing the smallest useful pixel size. At a 20 cm pixel size, it is probable that the brightness of pixels containing thar heads would increase by about 3.6. For thar observed from an aircraft, it is probable that pixel brightness would increase by a lesser factor, given that the area of head

visible from a vertical view would be less than from a front-on view. However, at least a factor of two increase in pixel brightness should be obtained by using pixels of about 20 cm size, even for an aircraft view. These calculations assume that a thar head is contained entirely within a single pixel. This is not an unreasonable assumption, since it is highly likely that while flying over thar a good percentage of the individual video frames will contain pixels which contain a whole head. (Similar observations can be made with possums: the possums 'twinkle' as the pixels within video frames alternate between covering only parts and then all the possum's body, resulting in varying pixel brightness.)

The effect of using a smaller pixel size on thar detection has been estimated for the thar observed in the alpine environment in this study. Data are given in Table 6. Eight times during the night we took the value of the single brightest (i.e. hottest) pixel observed for thar as representing the situation of thar facing the camera. This brightness value was then scaled according to the factor in Table 5 for the increase in brightness likely to be gained by using a 20 cm pixel size. The scaled value was then compared with the maximum brightness values (radiant temperatures) within the entire thermal image (values which would normally be associated with large rocks). As Table 6 shows, reducing the pixel size to 20 cm is likely to eliminate the confusion between thar and all other objects in the alpine environment during ground-based imaging, based on radiant temperature alone, over the entire period in which imaging was performed. That is, the scaled brightness values of pixels associated with thar greatly exceeds all other brightness values in the images. This continues to be true even when the data are scaled to represent detectability from an aircraft, when a reduction in the area of head visible to the camera will probably occur, but only for times from midnight onwards (see Table 6). We would not expect the reduced pixel size to increase the range of observed background (i.e. rock) temperatures, since only the larger rocks in the environment are hottest (they will cool most slowly), and these are almost certainly bigger than the nominal pixel size of 38 cm used for data collection in this study. Therefore, reducing the pixel size is not expected to have any effect on the maximum background temperatures observed. This expectation should be tested in any future study.

4.5 INCREASING THAR DETECTABILITY THROUGH IMAGE PROCESSING

The problem of detecting thar, or more precisely thar heads, in thermal imagery is similar to the problem of detecting possums. We have found several image processing operations that can decrease visual confusion between possums and other warm targets in a thermal image, and these are also expected to be effective for increasing detectability of thar. Although not required as part of this contract, we provide here an example of the best of these techniques: adaptive filtering. Adaptive filtering is a form of local contrast enhancement which enhances small bright objects on a darker background. It also helps remove the visual impact of larger bright objects in the thermal images. These objects will be rocks and not thar, and thus filtering simplifies the visual interpretation of the thermal image because there will be fewer targets to identify and reject.

The objective of any image enhancement operation is to reduce the number of pixels in the image that are brighter than the target of interest - in this case thar. Table 7 shows the results of applying an adaptive filter to the eight images for which data are given in Table 6. Comparing the columns which give the number of pixels brighter than (and thus confused with) thar, before and after filtering, shows that the adaptive filter offers a significant enhancement. Adaptive filtering alone reduces any confusion between thar and hot rocks to almost negligible levels in the TIR images acquired in the early morning (about 5 am onwards). Combining adaptive filtering of TIR images with small pixel sizes (ca. 20 cm) should enable thar to be unambiguously detected in alpine environment imagery on the basis of radiant temperature alone. At present we have no facilities to implement an adaptive filter to be applied to TIR video imagery in real-time as it is being played back to a video screen, but there is no technological impediment to doing so (although a significant development effort would be required).

5. Conclusions

Because of the rocky landscape, detection of thar in an alpine habitat using currently available TIR cameras is not without its challenges. Throughout the early evening, large rocks and bluffs remain warm, and mask any animals standing between these rocks and the camera because the radiant temperatures of the rocks exceed those of thar. Approximately six hours after sunset, the rocks have cooled sufficiently to allow easy detection of moving thar. However, sufficient hot rocks within the area covered by a typical TIR video image remain, so that stationary thar are not able to be detected, on the basis of radiant temperature alone, for the pixel sizes encountered in the alpine component of this study (pixels that image areas of about 38 cm square). Since the heads of thar are significantly hotter than their bodies, detectability is likely to be much increased by decreasing the area imaged by individual pixels in a TIR camera. Based on observations of thar radiant temperatures in this study, pixel sizes covering an area of about 20 cm square should be sufficiently small to allow unambiguous detection of stationary thar. The confusion between thar and warm rocks can also be greatly reduced by applying the standard image enhancement technique of adaptive filtering. The combination of smaller pixel sizes and image enhancement should make detection of thar using TIR imaging a robust technique. However, development of TIR cameras with larger numbers of pixels, and implementation of image enhancement in real-time during play-back of recorded TIR video, are both likely to be required before TIR imaging could be considered for operational estimation of thar populations.

The following particular conclusions are drawn from this study:

1. TIR imaging for detection of thar in an alpine environment should not be attempted until about six hours after sunset, to allow time for rocks to cool sufficiently. Ideally, imaging should be carried out from a few hours before dawn until about one hour after sunrise. At these times,

and under the conditions encountered in this study (thar at a distance such that pixel sizes of about 38 cm square were encountered), moving thar will be easily detected.

2. Under the conditions encountered in imaging thar in this study, stationary thar in the alpine environment could not be unambiguously detected on the basis of radiant temperature alone at any time during the night, because of overlap between the radiant temperature of thar and that of rocks. A smaller TIR imagery pixel size than that encountered in this study would be necessary to make detection unambiguous.

3. It is highly probable that stationary thar in an alpine environment could be detected with a high degree of reliability, on the basis of radiant temperature alone, if pixel sizes equivalent to imaging areas of 20 cm square could be used. These pixel sizes approximate the dimensions of a thar head, which is relatively hot. The certainty of detection can be further significantly increased by applying standard image enhancement techniques.

4. Thar moving in an alpine environment can probably be unambiguously detected with current TIR cameras operating from an aircraft, if the aircraft disturbs the animals and causes them to run about. However, cameras available in New Zealand will only allow limited swath widths to be covered (ca. 100 m). Cameras currently available overseas should be able to achieve swath widths of up to 300 m, for detection of moving thar. Future sensors should allow swath widths of up to 500 m, at ground speeds in excess of 120 km/hour. Aircraft safety may require that these cameras be used with long-telephoto lenses in an alpine environment, to gain flying height. This would require that the cameras be gyroscope-stabilised.

5. The use of TIR imaging for operational detection of thar has much in common with detection of possums, in terms of both the necessary developments in camera technology and the need to implement real time image enhancement of TIR video imagery to increase the certainty of detection. It should be possible to share the development cost of any operational system for TIR imaging across a range of animal population estimation applications (probably also including such animals as chamois, deer, seals, albatross, etc.).

6. Acknowledgements

Terry Farrell and Shane Cross of the Wild Animal Control Section of the West Coast Conservancy, Department of Conservation, are gratefully acknowledged for providing transport, supplies, and field assistance. The West Coast Conservancy, Department of Conservation is thanked for funding under Contract No. 2317.

James Shepherd of Landcare Research is thanked for modelling the rock cooling rates and plotting the diurnal cooling curve.

8. References

Best, R.G. 1981. Infrared emissivity and radiant surface temperatures of Canada and snow geese. *Journal of wildlife management* 45:1026-1029.

Birkebak, R.C., Birkebak, R.C. and Warner, D.W. 1964. A note on total emittance of animal integuments. *Journal of heat transfer.* Meeting of the American Soc. Mechanical Eng., Nov. 1963 Paper No 63-WA-20: 287-288.

Boonstra, R., Eadie J.M., Krebs, C.J. and Boutin, S. 1995. Limitations of far infrared thermal imaging in locating birds. *Journal of field ornithology* 66: 192-198.

Boonstra, R., Krebs, C.J., Boutin, S. and Eadie J.M. 1994. Finding mammals using far-infrared thermal imaging. *Journal of mammalogy* 75: 1063-1068.

Colwell, R.N. 1983 Manual of remote sensing (Vol. 1, 2nd Ed.).American Society of Photogrammetry, Falls Church. 1232pp.

Cowan, PE. 1990. Brushtail possum. In C.M. King, ed. The handbook of New Zealand mammals. Oxford Uni. Press. 600 pp.

Crampton, E.W, and Harris, L.E. 1969. Applied animal nutrition. W H. Freeman and Co., San Francisco. 753pp.

Croon, G.W., McCullough, D.R., Olson, C.E. and Queal, L.M. 1968. Infrared scanning techniques for big game censusing. *Journal of wildlife management* 32: 751-759.

Dawson, T.J. and Hulbert, A.J. 1970. Standard metabolism, body temperature, and surface areas of Australian marsupials. *American journal of physiology* 218: 1233-1238.

De Lamo, D.A. and Heath, J.E. 1985. Surface temperature regulation in Guanacos determined by thermography. *The physiologist* 28: 273.

Dymond, J.R. and Trotter, C.M. 1996. Remote sensing of possums using thermal infrared cameras. Landcare Research Contract Report LC9697/056.

Goody, R.M. and Yung,Y.L. 1989. Atmospheric radiation, Theoretical basis. 2nd Ed. Oxford University Press. 519 pp.

Forsyth, D.M. and Hickling, G.J. 1997. An improved technique for indexing abundance of Himalayan thar. *New Zealand journal of ecology* 21: 97-101.

Graves, H.B. and Ellis, E.D. 1972. Censusing white-tailed deer by airborne thermal infrared imagery. *Journal of wildlife management* 36: 875-884.

Guoquan, D. and Zhengzhi, L. 1992. The apparent emissivity of vegetation canopies. *International journal of remote sensing* 14: 183-188.

Halverson, G.J. 1994. Thermal imaging of opossums (sic) and other feral/wild animals. Report to the Animal Health Board, Wellington.

Kirkwood, J.J. and Cartwright,A. 1991: Comparisons of two systems for viewing bat behaviour in the dark. *Proceedings of the Indiana Academy of Science,* Vol. 102:133-137.

Klir, J.J. and Heath, J.E. 1992. An infrared thermographic study of surface temperature in relation to external thermal stress in three species of foxes: the red fox *(Vulpes vulpes),* Arctic fox (Alopex logopu), and kit fox *(Vulpes macrotis). Physiological* zoology 65: 1011-1021.

Korhonen, H. and Harri, M. 1986. Heat loss of farmed racoon dogs and blue foxes as evaluated by infrared thermography and body cooling. *Comparative biochemistry and physiology* 84A: 361-364.

Moen,A. 1968. Surface temperatures and radiant heat loss from white-tailed deer. *Journal of wildlife management* 31: 338-344.

Moen,A. 1973. Wildlife ecology, an analytical approach. W.H. Freeman and Co., San Francisco. 458 pp.

New Zealand Nautical Almanac 1997: Hydrographic Office of the Royal New Zealand Navy, Auckland. 191 p.

Sabol, B.M. and Hudson, M.K. 1995. Technique using thermal infrared imaging for estimating populations of gray bats. *Journal of mammalogy* 76: 1242-1248.

Sidle, J.G., Nagel, H.G., Clarke, R., Gilbert, C., Stuart, D., Willburn, K. and Orr, M. 1993. Aerial thermal infrared imaging of sandhill cranes on the Platte River, Nebraska. *Remote sensing of the environment* 43: 333-341.

Tustin, K.G. 1990. Pp 391-406 In King, Carolyn M. ed The Handbook of New Zealand Mammals. Oxford University Press Auckland, 600 p.

Watson, Kenneth 1971. Geologic Applications of Thermal Infrared Images. *Proceedings of the IEEE* January 1975 pp. 391-406.

Webb, P.I., Speakman,J.R. and Racey, P.A. 1993. The implication of small reductions in body temperature for radiant and convective heat loss in resting endothermic brown long-eared bats (*Plecotus auritus*). *Journal of thermal biology* 18: 131-135.

Wiggers, E.P and Beckerman, S.F. 1993. Use of thermal infrared sensing to survey white-tailed deer populations. *Wildlife society bulletin* 21: 263-268.

Table 1. Camera specifications (abbreviations: h - horizontal, v- vertical).

Prism DS TIR Camera	
Manufacturer	FLIR Systems Inc.
Wavelength range	3.6 - 5 um
Lens focal length	50 mm
Field of view (FOV)	9 ° x 7 °
Instantaneous FOV	0.48 milliradian
Detectors	PtSi hybrid silicon array
Resolution (hxv, pixels)	320 x 244
Temperature sensitivity	0.1 ° C
Cooling	Stirling

Table 2. Pixel sizes for the Prism DS camera with a 50 mm focal length camera lens, and the corresponding field sizes at varying distances from the camera. The field size (horizontal by vertical) gives the dimensions of the area viewed by the camera.

Distance (m)	Pixel size (mm)	Field size (h x v) (m)
100	48 x 48	12 x 15
200	96 x 96	23 x 31
400	192 x 192	47 x 62
600	288 x 288	70 x 92
800	384 x 384	94 x 123
1000	480 x 480	117 x 154

Table 3: Detection statistics. The maximum, minimum and median brightness levels of pixels representing thar were calculated from 48 separate sightings of thar, and are given in the first three columns. The second three columns show, for the three images containing the maximum, minimum, and median thar brightness levels, that 1%, 45%, and 2% of the total number of pixels in each image, respectively, were brighter than pixels representing thar. Even an image having 1% of background pixels with radiant temperatures greater than those of thar would lead to gross inaccuracies when estimating thar numbers, if these background pixels occurred in small groups of approximately thar-size.

Brightness levels of pixels representing thar (from 48 sightings)			Percentage of pixels with brightness levels greater than brightness levels associated with thar, for the three images with thar brightness levels equal to the maximum, minimum and median thar brightness levels observed during 48 sightings.		
Maximum	Minimum	Median	Maximum	Minimum	Median
125	44	85	1	45	2

Table 4: Dimensions of thar heads.

Animal	Area of head (cm^2)
Female	250
Male	400

Table 5: Areas of thar heads, and the proportions of the two pixel sizes occupied by them. Irrespective of whether it was male or female thar observed in the alpine imagery, it is probable that the brightness of the brightest pixels (those containing the head) would increase by a factor of about 3.6 if 20 cm pixels were used rather than the (nominally) 38 cm pixels encountered in this study.

Body part	Area (cm^2)	Percentage of pixel occupied by head for pixel of size:		Scaling factor
		38 by 38 cm	20 by 20 cm	
Female head	250	17	63	3.6
Male head	400	28	100	3.6

Table 6: Thar brightness levels taken from data obtained with 38 cm pixels and recalculated for 20 cm pixels, using the results from eight digitised frames imaged between 11.06 p.m. on 11 April and 8.15 p.m. on 12 April. Thar brightness levels are given in column two. Column three shows the maximum brightness levels in the image (the warmest rocks) and column four gives the number of pixels brighter than those associated with thar. The last two columns give re-calculated brightness levels for 20 cm square pixel sizes, similar to the head size of medium-sized animals. If the pixel brightness values are re-scaled to the conditions expected for an aerial view, (column six), the separation between the radiant temperature of thar and the background is not as great, but still sufficient from about midnight until 6.50 a.m. to distinguish thar easily from other objects.

Image time	Thar brightness levels (38 cm pixels)	Maximum brightness levels in image (large rocks)	Number of pixels brighter than thar	Thar brightness scaled for 20 cm pixels	Thar brightness scaled for 20 cm pixels and a vertical aerial view
23:06	99	154	2268	356	198
23:26	97	172	3420	349	194
23:51	125	182	476	450	250
04:57	107	126	137	385	214
05:28	73	92	35	263	146
05:44	97	120	136	349	194
06:50	84	98	81	302	168
08:13	117	242	100	421	234

Table 7: Comparison of the number of pixels in images of the alpine environment with brightness levels exceeding those of thar, with and without adaptive filtering, for eight images acquired at various times through the night. In each case the number of pixels brighter than thar is greatly reduced by filtering.

Image time	Unfiltered Max. thar brightness level	Max. image brightness level (rocks)	No. of pixels brighter than thar	Filtered Max. thar brightness level	Max. image brightness level (rocks)	No. of pixels brighter than thar
23:06	99	154	2268	125	185	665
23:26	97	172	3420	115	201	1652
23:51	125	182	476	160	214	147
04:57	107	126	137	155	165	3
05:28	73	92	35	109	111	1
05:44	97	120	136	137	152	2
06:50	84	98	81	128	121	0
08:13	117	129	100	148	140	0

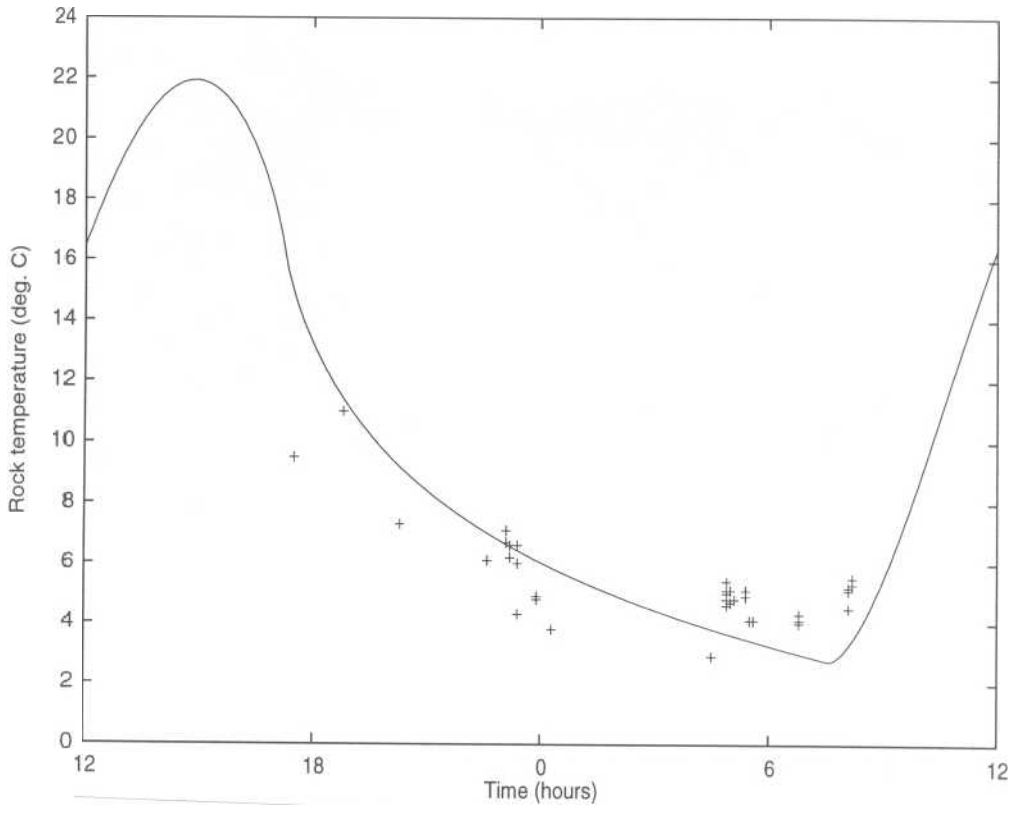

Figure 1: Diurual temperature curve derived from rock cooling, as modelled using the method of Watson (1975).

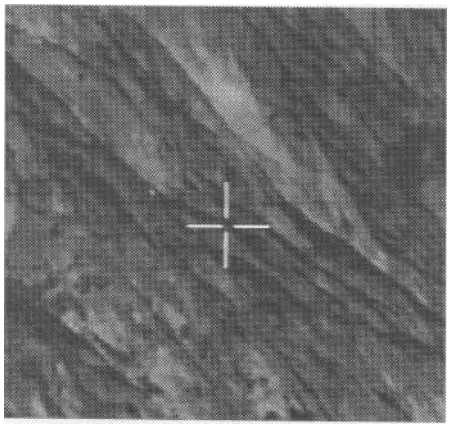

Figure 2: Subset of a digitised thermal video frame showing a view of a thar approximately 600 m from the camera. The thar is the small bright spot 10 mm to the left and 5 mm above the centre of the cross hairs. The area covered by the subset is approximately 3080 m^2. Note the considerable variation in brightness levels (radiant temperatures) over the area, which comprises rocky bluffs.

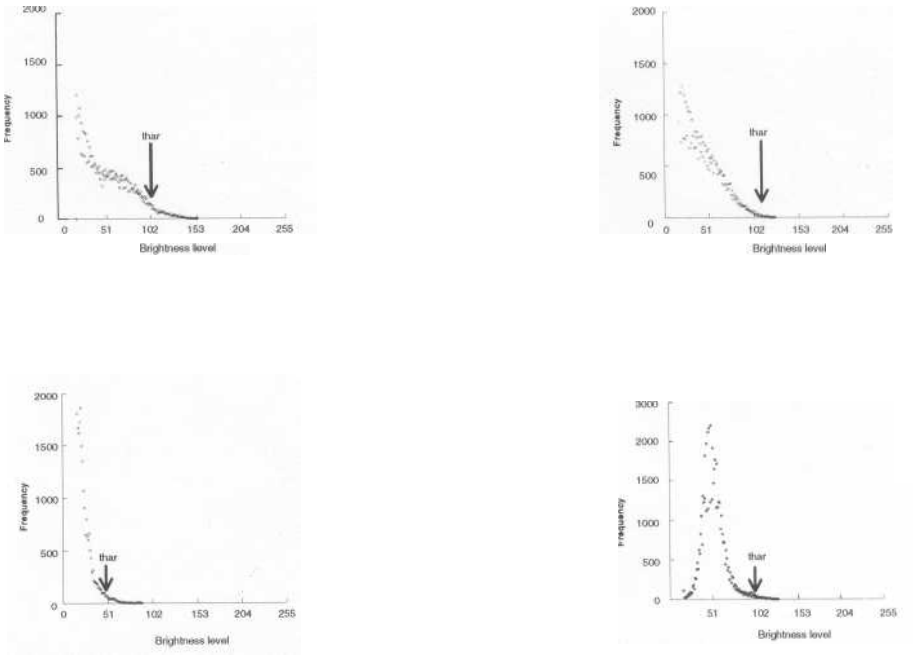

Figure 3: Plots of frequency (number of pixels) versus brightness levels (proportional to radiant temperature) for four images of thar in the alpine environment, acquired between 23.00 hours on 11 April and 08.15 hours on 12 April. The plots show the brightness levels of thar in relation to levels for background vegetation and rocks. The values of the pixels representing thar are indicated by the arrows, and indicate there is overlap between the brightness levels of rocks and thar. Brightness levels for vegetation occuply the left hand end of the curves, and rocks the right hand end.

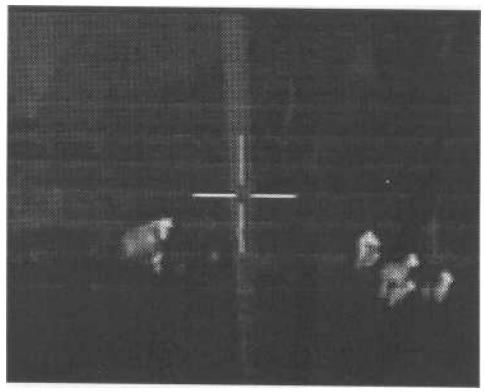

Figure 4: Subset of a digitised thermal video frame showing female and young thar on farmland, viewed at a range of approximately 150 m. Note the brighter heads and cooler bodies. Average head and body brightness levels correspond to a temperature difference of 3°C. The warm object in the foreground, immediately behind the cross hairs, is a fence-post, with the wires of the fence also visible.